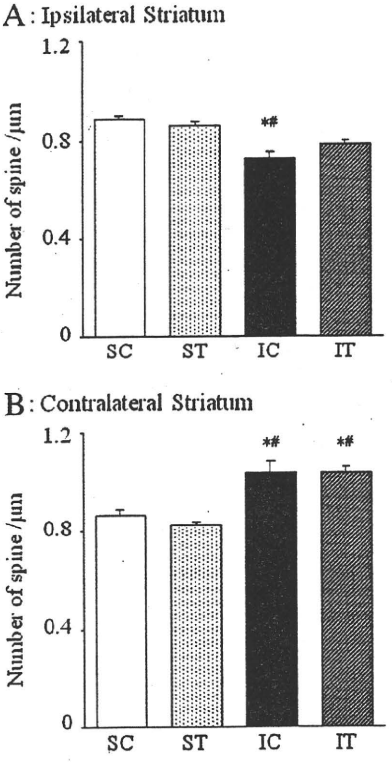

Fig. 6 – Spine density ipsilateral (A) and contralateral (B) to injured striatum 15 days after ICH. In the ipsilateral striatum, the spine density of IC was significantly lower than that of sham groups (SC, ST), but there were no differences between IT and sham groups (A). In the contralateral striatum, the spine density of ICH groups (IC, IT) was more than that of sham groups (SC, ST), but there was no difference between IC and IT (B). Values are represented as the mean ± SEM. $^{*}p<0.05$ compared with SC. $^{\#}p<0.05$ compared with ST. $^{\$}p<0.05$ compared with IC. SC: sham control group, ST: sham treadmill group, IC: ICH control group, IT: ICH treadmill group.

suggest that the improvement in motor function after treadmill running might result in alterations of dendritic morphology in the contralateral striatum after ICH.

4. Experimental procedures

4.1. *Animals models*

Male Wistar rats weighing 240–270 g (8 weeks of age) were used. Rats were housed at 25 °C during a 12 h light/dark cycle, with food and water made available ad libitum throughout the experiments. Animal care and surgical procedures were performed in accordance with the animal care guidelines of the Nagoya University. All efforts were made to minimize suffering and the number of animals used. They were randomly assigned to sham or ICH. Each group was divided into two subgroups: treadmill exercise and control (no exercise) groups. Therefore, four groups were included in this study: SC, ST, IC, and IT. Animals within each group were randomly assigned to three analysis groups: Hematoxylin–Eosin (H–E) staining, Golgi-Cox staining and Western blotting.

4.2. *Induction of ICH*

We used the bacterial collagenase model of ICH based on previous studies with minor modifications (Rosenberg et al., 1990; Del Bigio et al., 1996). To induce hemorrhage, rats were anesthetized with sodium pentobarbital (45 mg/kg, i.p.) and placed on a stereotaxic frame. Through a hole drilled in the skull, a needle (φ=400 μm) was implanted into the striatum at the following coordinates: 3.0 mm lateral to the midline, 0.2 mm anterior to the coronal suture, and depth 6.0 mm deep from the surface of the brain. 1.2 μl saline containing 0.24 U of collagenase (Type IV; Sigma-Aldrich, St. Louis, MO, USA) was infused over 6 min. The needle remained in place for an additional 7 min after the infusion and was subsequently withdrawn slowly. Sham operated animals were injected with 1.2 μl of saline instead of collagenase.

4.3. *Behavioral testing*

Motor behavior was evaluated using four tests in each rat from days 1 to 15 after ICH induction. The specific tests included (1) observation of spontaneous ipsilateral circling, graded from 0 (no circling) to 3 (continuous circling); (2) contralateral hindlimb retraction, which measured the ability of the animal to replace the hindlimb after it was displaced laterally by 2–3 cm, graded from 0 (immediate replacement) to 3 (replacement after minutes or no replacement); (3) beam walking ability, graded 0 for a rat that readily traverses a 2.4-cm-wide, 80-cm-long beam to 3 for a rat unable to stay on the beam for 10 s; and (4) bilateral forepaw grasp, which measures the ability to hold onto a 2-mm diameter steel rod, graded 0 for a rat with normal forepaw grasping behavior to 3 for a rat unable to grasp with the forepaws. The scores from all four tests were added to give a motor deficit score (MDS; maximum possible score, 12) (Altumbabic et al., 1998).

4.4. *Treadmill exercise*

Animals in the treadmill groups (ST and IT) were forced to run on a motorized treadmill for 30 min at a speed of 9 m/min once a day. The treadmill groups were scheduled to run on a treadmill from days 4 to 14 after ICH induction, 11 consecutive days. Animals in the control groups (SC and IC) were left in the treadmill without running for the same period as the treadmill groups. All animals were forced to run after behavioral tests had finished.

4.5. *H–E staining*

At 15 days after surgery, animals (SC, n=8; ST, n=8; IC, n=6; IT, n=7) were randomly selected, placed under deep anesthesia with sodium pentobarbital (45 mg/kg, i.p.), transcardially perfused with 0.9% saline, and subsequently

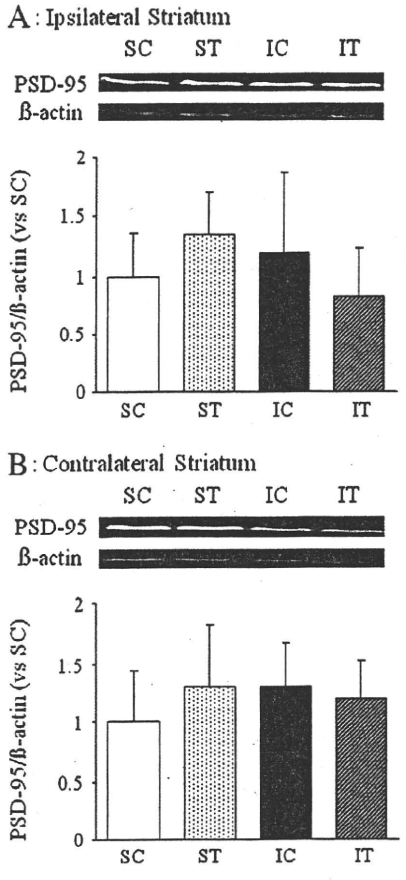

Fig. 7 – PSD-95 protein level measured by Western blot both ipsilateral (A) and contralateral (B) to injured striatum 15 days after ICH. PSD-95 levels were normalized to β-actin and expressed as percentage of SC. The PSD-95 protein level of ST was highest among the four groups, but there were no significantly differences between the groups. Values are represented as the mean ± SEM. SC: sham control group, ST: sham treadmill group, IC: ICH control group, IT: ICH treadmill group.

fixed with phosphate buffer (pH 7.4) containing 4% paraformaldehyde. The brains were removed and postfixed in the same fixative for 5 days. Then, 40 μm thick coronal sections were obtained using a cryostat after overnight cytoprotection in 30% sucrose solution. These sections were stained with H–E.

Volume of tissue lost in the striatum was determined using Scion Image (Scion Corporation, Frederick, MD, USA) by measuring the area of striatum remaining in eight sections spaced 400 μm apart ranging from +1.7 to −1.5 mm to bregma. All the hemorrhagic tissue induced by the surgery was included within the range.

Volume of a striatum = average (area of coronal section of the striatum − area of damage) × section interval × number of sections.

Volume of tissue lost (%) = (remaining volume of non-injured striatum − remaining volume of injured striatum)/ remaining volume of non-injured striatum.

4.6. *Golgi-Cox staining*

At 15 days after surgery, animals (SC, $n=7$; ST, $n=7$; IC, $n=6$; IT, $n=6$) were randomly selected, placed under deep anesthesia with sodium pentobarbital (45 mg/kg, i.p.), and transcardially perfused with 0.9% saline. Extracted brains were stored in Golgi-Cox solution for 14 days in the dark. The brains were then immersed in 30% sucrose solution for another 2 days before sectioning. Coronal brain sections were cut using a vibratome at 200 μm and developed as previously described (Gibb and Kolb, 1998).

Six medium-sized spiny neurons in the ipsilateral (peri-hematoma lesion) and contralateral striatum taken from a coronal section between 0 and 1.7 mm anterior to the bregma were selected at random per animal. Dendritic arborization and length was analyzed by Sholl analysis, which examines the number of intersections of dendritic branches and rings, at 20 μm intervals from the cell body (Sholl, 1956; Biernaskie and Corbett, 2001; Campaña et al., 2008). Spine density (number of spines/μm dendrite) was calculated by dividing the total number of laterally oriented spines by the length of the dendrite from medium-sized spiny neurons (Brown et al., 2008; Campaña et al., 2008).

4.7. *Western blotting*

At 15 days after surgery, animals (SC, $n=7$; ST, $n=7$; IC, $n=6$; IT, $n=6$) were randomly selected, placed under deep anesthesia with sodium pentobarbital (45 mg/kg, i.p.), transcardially perfused with phosphate buffered saline (PBS, pH 7.4), and their brains removed. Briefly, brains were dissected on ice into ipsilateral or contralateral striatum blocks and rapidly frozen on dry ice. Brain samples were homogenized with ice cold lysis buffer (50 mM Tris–HCl, 150 mM NaCl, 2 mM EDTA, 0.2% Triton X-100, 0.2% NP40) containing protease inhibitors (Complete, Roche, Mannheim, Germany). Samples were centrifuged at 15,000 rpm at 4 °C for 30 min. Protein concentrations were determined using a BCA Protein Assay Kit (Thermo Scientific, Rockford, IL, USA). Equal volumes (20 μm) of protein extracts from brain tissue were resolved by electrophoresis through a 12% polyacrylamide gel under reducing conditions and then transferred to a PVDF membrane (ATTO Corporation, Tokyo, Japan). Membranes were blocked with 5% skim milk in TBST buffer. PSD-95 (1:2000, Sigma-Aldrich) and β-actin (1:2000, Sigma-Aldrich) primary antibody was then added to membranes and allowed to incubate overnight at 4 °C, followed by HRP secondary antibodies (1:1000, Cell Signaling Technology, Danvers, MA, USA) for 2 h room temperature. After rinsing with buffer, the immunocomplexes were visualized using standard chemical luminescence methods (ECL plus, GE Healthcare, Buckinghamshire, UK). The film signals were digitally scanned and quantified using densitometric image software (CS Analyzer, ATTO Corporation), normalized for β-actin level.

4.8. *Statistical analysis*

Kruskal–Wallis and Mann–Whitney U-test were used for analysis of MDS. One-way ANOVA and Tukey's post hoc

comparison was used for analysis of the volume of tissue lost in the striatum, dendritic arborization and length, spine density and PSD-95 protein level between each groups. The criterion for significance was set at $p<0.05$.

Acknowledgment

This study was supported by JSPS Grant-in-Aid for Scientific Research (22500456).

REFERENCES

Altumbabic, M., Peeling, J., Del Bigio, M.R., 1998. Intracerebral hemorrhage in the rat: effects of hematoma aspiration. Stroke 29, 1917–1923.

Ang, E.T., Wong, P.T., Moochhala, S., Ng, Y.K., 2003. Neuroprotection associated with running: is it a result of increased endogenous neurotrophic factors? Neuroscience 118, 335–345.

Biernaskie, J., Corbett, D., 2001. Enriched rehabilitative training promotes improved forelimb motor function and enhanced dendritic growth after focal ischemic injury. J. Neurosci. 21, 5272–5280.

Brown, C.E., Wong, C., Murphy, T.H., 2008. Rapid morphologic plasticity of peri-infarct dendritic spines after focal ischemic stroke. Stroke 39, 1286–1291.

Bury, S.D., Adkins, D.L., Ishida, J.T., Kotzer, C.M., Eichhorn, A.C., Jones, T.A., 2000. Denervation facilitates neuronal growth in the motor cortex of rats in the presence of behavioral demand. Neurosci. Lett. 287, 85–88.

Calautti, C., Baron, J.C., 2003. Functional neuroimaging studies of motor recovery after stroke in adults: a review. Stroke 34, 1553–1566.

Campaña, A.D., Sanchez, F., Gamboa, C., Gómez-Villalobos Mde, J., De La Cruz, F., Zamudio, S., Flores, G., 2008. Dendritic morphology on neurons from prefrontal cortex, hippocampus, and nucleus accumbens is altered in adult male mice exposed to repeated low dose of malathion. Synapse 62, 283–290.

Chang, H.C., Yang, Y.R., Wang, S.G., Wang, R.Y., 2009. Effects of treadmill training on motor performance and extracellular glutamate level in striatum in rats with or without transient middle cerebral artery occlusion. Behav. Brain Res. 205, 450–455.

Del Bigio, M.R., Yan, H.J., Buist, R., Peeling, J., 1996. Experimental intracerebral hemorrhage in rats. Magnetic resonance imaging and histopathological correlates. Stroke 27, 2312–2320.

Dietrich, M.O., Mantese, C.E., Porciuncula, L.O., Ghisleni, G., Vinade, L., Souza, D.O., Portela, L.V., 2005. Exercise affects glutamate receptors in postsynaptic densities from cortical mice brain. Brain Res. 1065, 20–25.

Gibb, R., Kolb, B., 1998. A method for vibratome sectioning of Golgi-Cox stained whole rat brain. J Neurosci Methods. 79, 1–4.

Han, K., Kim, E., 2008. Synaptic adhesion molecules and PSD-95. Prog. Neurobiol. 84, 263–283.

Hu, S., Ying, Z., Gomez-Pinilla, F., Frautschy, S.A., 2009. Exercise can increase small heat shock proteins (sHSP) and pre- and post-synaptic proteins in the hippocampus. Brain Res. 1249, 191–201.

Johansson, B.B., 2000. Brain plasticity and stroke rehabilitation. The Willis lecture. Stroke. 31, 223–230.

Jones, T.A., Schallert, T., 1992. Overgrowth and pruning of dendrites in adult rats recovering from neocortical damage. Brain Res. 581, 156–160.

Jones, T.A., Schallert, T., 1994. Use-dependent growth of pyramidal neurons after neocortical damage. J. Neurosci. 14, 2140–2152.

Jones, T.A., Kleim, J.A., Greenough, W.T., 1996. Synaptogenesis and dendritic growth in the cortex opposite unilateral sensorimotor cortex damage in adult rats: a quantitative electron microscopic examination. Brain Res. 733, 142–148.

Kato, S., Masuda, T., Hida, H., Ishida, K., Ida, K., Nishino, H., 2004. The effect of treadmill running on motor cortex thickness after intracerebral hemorrhage in rats. Neurosc Res. 50 S95, P1-224 (Abstract).

Kim, M.W., Bang, M.S., Han, T.R., Ko, Y.J., Yoon, B.W., Kim, J.H., Kang, L.M., Lee, K.M., Kim, M.H., 2005. Exercise increased BDNF and trkB in the contralateral hemisphere of the ischemic rat brain. Brain Res. 1052, 16–21.

Kleim, J.A., Jones, T.A., Schallert, T., 2003. Motor enrichment and the induction of plasticity before or after brain injury. Neurochem. Res. 28, 1757–1769.

Langhorne, P., Holmqvist, L.W., 2007. Early supported discharge after stroke. J. Rehabil. Med. 39, 103–108.

Langhorne, P., Taylor, G., Murray, G., Dennis, M., Anderson, C., Bautz-Holter, E., Dey, P., Indredavik, B., Mayo, N., Power, M., Rodgers, H., Ronning, O.M., Rudd, A., Suwanwela, N., Widen-Holmqvist, L., Wolfe, C., 2005. Early supported discharge services for stroke patients: a meta-analysis of individual patients' data. Lancet 365, 501–506.

Lee, H.H., Kim, H., Lee, M.H., Chang, H.K., Lee, T.H., Jang, M.H., Shin, M.C., Lim, B.V., Shin, M.S., Kim, Y.P., Yoon, J.H., Jeong, I.G., Kim, C.J., 2003. Treadmill exercise decreases intrastriatal hemorrhage-induced neuronal cell death via suppression on caspase-3 expression in rats. Neurosci. Lett. 352, 33–36.

Lee, H.H., Shin, M.S., Kim, Y.S., Yang, H.Y., Chang, H.K., Lee, T.H., Kim, C.J., Cho, S., Hong, S.P., 2005. Early treadmill exercise decreases intrastriatal hemorrhage-induced neuronal cell death and increases cell proliferation in the dentate gyrus of streptozotocin-induced hyperglycemic rats. J Diabetes Complications 19, 339–346.

Lou, S.J., Liu, J.Y., Chang, H., Chen, P.J., 2008. Hippocampal neurogenesis and gene expression depend on exercise intensity in juvenile rats. Brain Res. 1210, 48–55.

McAllister, A.K., Katz, L.C., Lo, D.C., 1999. Neurotrophins and synaptic plasticity. Annu. Rev. Neurosci. 22, 295–318.

Metz, Gerlinde A., Whishaw, Ian Q., 2002. Cortical and subcortical lesions impair skilled walking in the ladder rung walking test: a new task to evaluate fore- and hindlimb stepping, placing, and co-ordination. J Neurosci Methods. 115, 169–179.

Molteni, R., Ying, Z., Gómez-Pinilla, F., 2002. Differential effects of acute and chronic exercise on plasticity-related genes in the rat hippocampus revealed by microarray. Eur. J. Neurosci. 16, 1107–1116.

Montoya, C.P., Campbell-Hope, L.J., Pemberton, K.D., Dunnett, S.B., 1991. The "staircase test": a measure of independent forelimb reaching and grasping abilities in rats. J Neurosci Methods 36, 219–228.

Nguyen, A.P., Huynh, H.D., Sjovold, S.B., Colbourne, F., 2008. Progressive brain damage and alterations in dendritic arborization after collagenase-induced intracerebral hemorrhage in rats. Curr. Neurovasc. Res. 5, 171–177.

Noskin, O., Krakauer, J.W., Lazar, R.M., Festa, J.R., Handy, C., O'Brien, K.A., Marshall, R.S., 2008. Ipsilateral motor dysfunction from unilateral stroke: implications for the functional neuroanatomy of hemiparesis. J. Neurol. Neurosurg. Psychiatry 79, 401–406.

Park, J.W., Bang, M.S., Kwon, B.S., Park, Y.K., Kim, D.W., Shon, S.M., Jeong, S.W., Lee, D.K., Kim, D.E., 2010. Early treadmill training promotes motor function after hemorrhagic stroke in rats. Neurosci. Lett. 471, 104–108.

Redila, V.A., Christie, B.R., 2006. Exercise-induced changes in

dendritic structure and complexity in the adult hippocampal dentate gyrus. Neuroscience 137, 1299–1307.
Risedal, A., Zeng, J., Johansson, B.B., 1999. Early training may exacerbate brain damage after focal brain ischemia in the rat. J. Cereb. Blood Flow Metab. 19, 997–1003.
Rosenberg, G.A., Mun-Bryce, S., Wesley, M., Kornfeld, M., 1990. Collagenase-induced intracerebral hemorrhage in rats. Stroke 21, 801–807.
Sheng, M., Hoogenraad, C.C., 2007. The postsynaptic architecture of excitatory synapses: a more quantitative view. Annu. Rev. Biochem. 76, 823–847.
Sheng, M., Kim, M.J., 2002. Postsynaptic signaling and plasticity mechanisms. Science 298, 776–780.
Sholl, D.A., 1956. The measurable parameters of the cerebral cortex and their significance in its organization. Prog. Neurobiol. 2, 324–333.
Soya, H., Nakamura, T., Deocaris, C.C., Kimpara, A., Iimura, M., Fujikawa, T., Chang, H., McEwen, B.S., Nishijima, T., 2007. BDNF induction with mild exercise in the rat hippocampus. Biochem. Biophys. Res. Commun. 358, 961–967.
Stranahan, A.M., Khalil, D., Gould, E., 2007. Running induces widespread structural alterations in the hippocampus and entorhinal cortex. Hippocampus 17, 1017–1022.
Sudlow, C.L., Warlow, C.P., 1997. Comparable studies of the incidence of stroke and its pathological types: results from an international collaboration. International Stroke Incidence Collaboration. Stroke 28, 491–499.
Teasell, R., Bayona, N., Salter, K., Hellings, C., Bitensky, J., 2006. Progress in clinical neurosciences: stroke recovery and rehabilitation. Can. J. Neurol. Sci. 33, 357–364.
Thorsén, A.M., Holmqvist, L.W., de Pedro-Cuesta, J., von Koch, L., 2005. A randomized controlled trial of early supported discharge and continued rehabilitation at home after stroke: five-year follow-up of patient outcome. Stroke 36, 297–302.
Whishaw, I., Pellis, S.M., 1990. The structure of skilled forelimb reaching in the rat: a proximally driven movement with a single distal rotatory component. Behav. Brain Res. 41, 49–59.
Yang, Y.R., Wang, R.Y., Wang, P.S., 2003. Early and late treadmill training after focal brain ischemia in rats. Neurosci. Lett. 339, 91–94.
Yoshii, A., Constantine-Paton, M., 2007. BDNF induces transport of PSD-95 to dendrites through PI3K-AKT signaling after NMDA receptor activation. Nat. Neurosci. 10, 702–711.

Bioorganic & Medicinal Chemistry Letters 20 (2010) 5126–5129

Contents lists available at ScienceDirect

Bioorganic & Medicinal Chemistry Letters

journal homepage: www.elsevier.com/locate/bmcl

S-Benzylisothiourea derivatives as small-molecule inhibitors of indoleamine-2,3-dioxygenase

Kenji Matsuno [a], Kazushige Takai [a], Yoshinobu Isaka [a], Yuka Unno [a], Masayuki Sato [a], Osamu Takikawa [b], Akira Asai [a,*]

[a] Graduate School of Pharmaceutical Sciences, University of Shizuoka, 52-1 Yada, Suruga-ku, Shizuoka 422-8526, Japan
[b] National Institute for Longevity Sciences, National Center for Geriatrics and Gerontology, 36-3 Gengo, Morioka, Obu, Aichi 474-8522, Japan

ARTICLE INFO

Article history:
Received 16 March 2010
Revised 25 June 2010
Accepted 7 July 2010
Available online 11 July 2010

Keywords:
SAR
IDO
Tryptophan
Kynurenine
Cancer

ABSTRACT

S-Benzylisothiourea **3a** was discovered by its ability to inhibit indoleamine-2,3-dioxygenase (IDO) in our screening program. Subsequent optimization of the initial hit **3a** lead to the identification of sub-μM inhibitors **3r** and **10h**, both of which suppressed kynurenine production in A431 cells. Synthesis and structure–activity relationship of S-benzylisothiourea analogues as small-molecule inhibitors of IDO are described.

Indoleamine 2,3-dioxygenase (IDO) is an extrahepatic heme-containing dioxygenase that catalyzes the addition of oxygen across the C-2/C-3 bond of the indole ring of tryptophan (Trp).[1,2] This is the initial and rate-limiting step in the catabolism of the essential amino acid Trp to *N*-formylkynurenine along the kynurenine pathway, which leads to biologically active metabolites such as the neurotransmitter serotonin, excitoxin quinolinic acid, *N*-methyl-D-aspartate (NMDA) receptor antagonist kynurenic acid, and nicotinamide adenine dinucleotide (NAD).[3–5]

IDO is expressed ubiquitously but predominately in cells within the immune system where it is specifically induced in dendritic cells and macrophages at the sites of inflammation by cytokines.[1] It is known that IDO is overexpressed in a variety of diseases, including cancer,[6] neurodegenerative disorders (e.g., Alzheimer's disease),[7] age-related cataract,[8] and HIV encephalitis.[9] Among these, IDO has been shown to play an important role in the process of immune escape by tumors.[1] In environments where the Trp concentration has been depleted by IDO, killer T cells cannot be activated by antigens, and they undergo G1 cell cycle arrest leading to apoptosis and immunosuppression.[10] Consequently, tumor cells escape from the immune response and survive. This is consistent with the observation that increased expression of IDO in tumor cells is correlated with poor prognosis for survival in patients with serious ovarian and colorectal cancers.[11,12]

Several IDO inhibitors have been reported to date (Chart 1). 1-Methyltryptophan (1-MT) is the most frequently used inhibitor with a weak K_i of 34 μM and is in clinical development at the National Cancer Institute.[13–15] The natural product brassinin, which possesses a dithiocarbamate group, has been reported to be a weak IDO inhibitor (K_i >10 μM).[16] In 2008–2009, naphthoquinones (e.g., menadione),[17] exiguamine A,[18] phenylimidazoles **1**,[19] and 4-amino-1,2,5-oxadiazole-3-carboximidamide **2**[20] were newly reported as IDO inhibitors, some of which exhibited in vivo efficacy to reveal preclinical proof of concept (POC) of IDO inhibition in

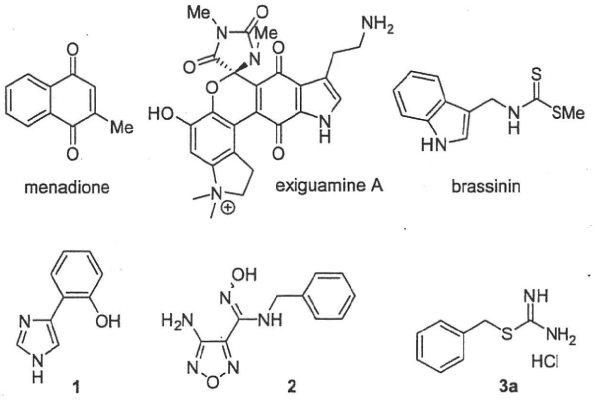

Chart 1. IDO inhibitors.

* Corresponding author.
E-mail address: aasai@u-shizuoka-ken.ac.jp (A. Asai).

0960-894X/$ - see front matter © 2010 Elsevier Ltd. All rights reserved.
doi:10.1016/j.bmcl.2010.07.025

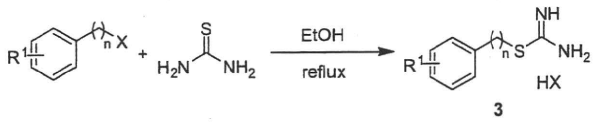

Scheme 1. Preparation of isothioureas **3**.

cancer treatment. The combination of menadione (also known as vitamin K_3) with the cytotoxic agent paclitaxel led to regression of tumors in mouse models (e.g., MMTV-Neu transgenic and B16-F10 xenograft) that showed no response to the cytotoxin administered alone.[17] A similarly positive in vivo response has been obtained by using siRNA to silence the IDO gene in B16-F10 tumor-bearing mice.[21] By screening campaign for our chemical library, we have also found that the *S*-benzylisothiourea derivative **3a** is an IDO inhibitor. Herein we report the structure–activity relationship (SAR) for IDO inhibition including cellular activity; specifically, we investigated substituents on the benzene ring, and modification of the linker to and replacement of the isothiourea moiety including isosters. In addition, we carried out kinetic analysis of *S*-benzylisothiourea analogues.

The tested compounds were purchased from commercial sources or synthesized. The isothioureas **3** were obtained by alkylation of thiourea with the corresponding phenylalkyl halide (Scheme 1). Treatment of iso(thio)cyanate with ammonia provided the (thio)ureas (**6** and **7**).

The inhibitory activity of the isothioureas **3** on human IDO is listed in Table 1.[22] For the *S*-benzylisothiourea series (**3a–3s**), the substituent on the benzene ring was found to be important for IDO inhibition; incorporation of 2-Cl (**3b**) enhanced inhibitory activity, and the 3-Cl (**3c**) and 4-Cl (**3d**) analogues were more potent inhibitors. Among the 4-substituted-*S*-benzylisothioureas, the 4-Br (**3f**) and 4-CF_3 (**3k**) analogues retained potent activity, while replacement with 4-F (**3e**), 4-Me (**3g**), 4-Et (**3h**), 4-OMe (**3l**), 4-CN (**3m**), and 4-NO_2 (**3n**) reduced activity. Moreover, analogues with 4-*i*Pr (**3i**), 4-*tert*-Bu (**3j**), 4-SO_2Me (**3p**), 4-COPh (**3q**), and 4-COOH (**3o**) were completely inactive; IDO disfavored bulky and hydrophilic substituents at this position. Further addition of 2-Cl to *S*-(4-chlorobenzyl)isothiourea **3d** resulted in sub-μM inhibition (**3r**); however, further addition of 3-Cl (**3s**) reduced activity. The SAR with respect to the position of the Cl atom of chlorophenethylisothioureas (**3t–3v**) was similar to that of chlorobenzylisothioureas, namely, 4-Cl (**3v**) was rather potent, but the inhibitory activity was substantially reduced. These results indicate that the halogen atom might play an important role in the interaction with IDO, which was recently found to make an important contribution to protein–ligand binding affinity,[23] and the distance from the isothiourea moiety is crucial for the inhibitory activity. The potent analogues are still small; they have an high ligand efficiency (LE)[24], that is, LE = 0.67 for compound **3r**.

All analogues were also evaluated for kynurenine production in human epithelial carcinoma A431 cells (Table 1).[25] In this cell line, there observed up-regulation of IDO and increased production of kynurenine by stimulation with interferon-γ (IFN-γ) (Fig. 1).[26] The potent IDO inhibitors displayed inhibition of kynurenine production with an SAR similar to that for IDO inhibition. Most of the compounds demonstrated slightly more potent activity in the A431 cell assay than in the IDO enzyme assay, as in a previous report.[20] This result was presumably due to the complexity of the IDO enzyme assay with a regeneration system of IDO in its active Fe^{2+} form, or due to the difference between recombinant IDO in the enzyme assay and endogenous IDO in the A431 cells. Furthermore, compound **3d** suppressed kynurenine production without reduction of IDO expression at 10 μM, which is higher concentration than IC_{50} value (Fig. 1).

Table 1
Inhibitory activity of benzylthioureas **3** and compounds **4–12**

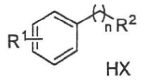

Compound	R^1	*n*	R^2	HX	IC_{50}, μM	
					IDO	A431[a]
3a	H	1	SC(=NH)NH_2	HCl	61	>10
3b	2-Cl	1	SC(=NH)NH_2	HCl	10	4.8
3c	3-Cl	1	SC(=NH)NH_2	HCl	4.6	1.4
3d	4-Cl	1	SC(=NH)NH_2	HCl	2.2	0.6
3e	4-F	1	SC(=NH)NH_2	HCl	13	2.0
3f	4-Br	1	SC(=NH)NH_2	HBr	1.3	0.8
3g	4-Me	1	SC(=NH)NH_2	HCl	30	6.8
3h	4-Et	1	SC(=NH)NH_2	HCl	16	2.5
3i	4-*i*Pr	1	SC(=NH)NH_2	HBr	>100	>20
3j	4-*tert*-Bu	1	SC(=NH)NH_2	HBr	>100	>20
3k	4-CF_3	1	SC(=NH)NH_2	HCl	2.6	1.2
3l	4-OMe	1	SC(=NH)NH_2	HCl	52	10
3m	4-CN	1	SC(=NH)NH_2	HBr	19	2.6
3n	4-NO_2	1	SC(=NH)NH_2	HCl	11	2.2
3o	4-COOH	1	SC(=NH)NH_2	HCl	>100	>20
3p	4-SO_2Me	1	SC(=NH)NH_2	HBr	>100	>10
3q	4-COPh	1	SC(=NH)NH_2	HBr	>100	>20
3r	2,4-Cl_2	1	SC(=NH)NH_2	HBr	0.4	1.1
3s	3,4-Cl_2	1	SC(=NH)NH_2	HCl	17	7.3
3t	2-Cl	2	SC(=NH)NH_2	HBr	>100	>20
3u	3-Cl	2	SC(=NH)NH_2	HBr	>100	>20
3v	4-Cl	2	SC(=NH)NH_2	HBr	57	>20
4	4-Cl	1	SC(=NMe)NHMe	$HClO_4$	21	>20
5a	4-Cl	0	NHC(=NH)SMe	HI	>100	>20
5b	4-Cl	2	NHC(=NH)SMe	HI	>100	>20
6a	4-Cl	0	$NHCSNH_2$	None	>100	>20
6b	4-Cl	2	$NHCSNH_2$	None	100	>20
7	4-Cl	1	$NHCONH_2$	None	>100	>20
8a	4-Cl	1	NH_2	None	>100	>20
8b	4-Cl	2	NH_2	None	>100	>20
9	4-Cl	1	OH	None	>100	>20
10a	4-Cl	1	SH	None	3.2	1.1
10b	2-Cl	1	SH	None	1.2	15
10c	H	1	SH	None	1.7	13
10d	4-F	1	SH	None	1.8	1.9
10e	4-Me	1	SH	None	1.3	6.5
10f	4-OMe	1	SH	None	1.4	9.4
10g	2,4-Cl_2	1	SH	None	3.5	4.6
10h	3,4-Cl_2	1	SH	None	0.1	1.1
10i	4-Cl	0	SH	None	1.9	>20
11	4-Cl	0	SO_2Na	None	>100	>20
12	4-Cl	0	SO_3H	None	>100	>20

[a] Kynurenine production in A431 cells.

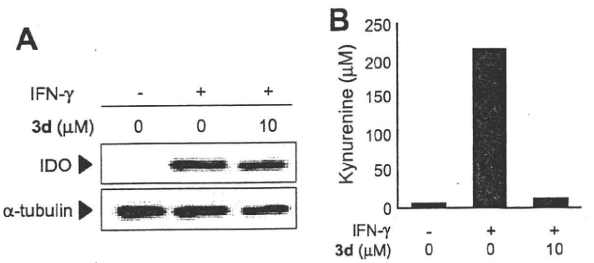

Figure 1. Effects of compound **3d** on IDO expression and kynurenine production in A431 cells stimulated with IFN-γ. (A) Western blot analysis of IDO in cell lysate from A431 cells. (B) Kynurenine concentration in culture medium.

Next, modification of the isothiourea moiety was investigated (Table 1). Bis-methylation of the N atoms (**4**) of isothiourea reduced inhibitory activity. *N*-4-Chlorophenyl (**5a**) and *N*-4-chlorophenethyl (**5b**) isothioureas were completely inactive. Also, replacement with thioureido (**6a** and **6b**), ureido (**7**), amino (**8a**

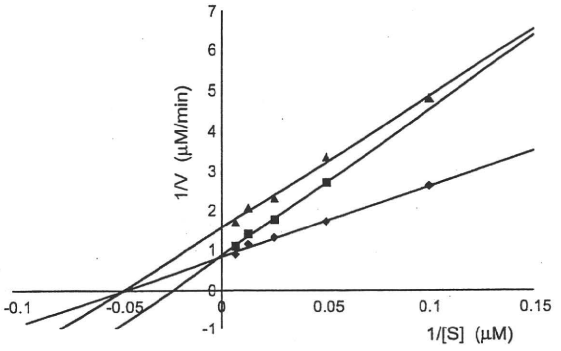

Figure 2. Steady-state kinetic analysis of recombinant human IDO by Lineweaver–Burk plot. ♦ No inhibition, ■ L-1-MT (100 μM), and ▲ compound **3d** (1 μM).

and **8b**) and hydroxyl (**9**) groups resulted in total loss of activity. On the contrary, the benzylthiols (**10a–10h**) showed potent inhibitory activity both for IDO and kynurenine production in A431 cells. With respect to the substituents on the phenyl ring, the SARs differed from those of the benzylisothioureas **3**; 4-Cl (**10a**) was also a potent inhibitor, and 2-Cl (**10b**), H (**10c**), 4-F (**10d**), 4-Me (**10e**), and 4-OMe (**10f**) retained similarly potent inhibitory activity, unlike the corresponding benzylisothioureas **3**. For incorporation of an additional Cl atom (**10g** and **10h**), 2,4-Cl_2 (**10g**) was equipotent to the parent 4-Cl (**10a**), and 3,4-Cl_2 (**10h**) exhibited the most potent IDO inhibition (IC_{50} = 0.1 μM), in contrast with the corresponding isothioureas (**3r** and **3s**). 4-Chlorobenzenethiol (**10i**), which did not include the methylene chain of 4-chlorobenzylthiol (**10a**), exhibited similarly potent inhibitory activity for IDO; however, no cellular inhibition of kynurenine production in A431 cells was observed. This might be due to cellular penetration issues caused by different physicochemical properties such as the stronger pK_a value of the benzenethiol. Analogues with SO_2Na (**11**) and SO_3H (**12**), which are oxidized forms of SH, were completely inactive.

Compound **3d** was selected for further kinetic studies. As shown in Figure 2, the Lineweaver–Burk plot was found to be consistent with an noncompetitive inhibition mode, unlike exiguamine A derivatives with uncompetitive inhibition[18] or 4-amino-1,2,5-oxadiazole-3-carboximidamide with competitive inhibition.[20] In this experiment, L-1-MT exhibited competitive inhibition that was the same as reported in the literature.[27]

The distinct SARs between benzylisothioureas **3** and benzylthiols **10** might be due to differing binding modes in the heme region at the active site of IDO, since noncompetitive inhibitors could also bind at alternative pockets around the active site of IDO.[28,29] Given the well-known metal coordinating properties of SH, it is likely that the SH moiety of benzylthiol chelates to the heme iron. In similar fashion, the isothiourea may bind to heme itself. Alternatively, the isothiourea could be a good bidentate acceptor of carboxylic acid. Since there are propionic acid in the heme structure, and some amino acid residues of carboxylic acid such as Asp274 and Glu171 around the active site,[30] we speculate that the isothiourea moiety interacts with such carboxylic acid. This speculation is supported by the reduction in IDO inhibition for bis-methylated *S*-isothioureas (**4**) and *N*-isothioureas (**5a** and **5b**). Further analysis to clarify the molecular interaction of those compounds with IDO is in progress.

In conclusion, we have identified the benzylisothiourea analogues **3** as novel noncompetitive IDO inhibitors by our screening campaign, derivatization and kinetic analysis. The 4-Cl/Br atom on the phenyl ring and the distance from the isothiourea moiety were important for potent IDO inhibition. Replacements of the isothiourea moiety afforded potent benzylthiol analogues with SARs that were distinct from those of the benzylisothioureas. Most of the potent IDO inhibitors also suppressed kynurenine production in A431 cells, with the exception of benzenethiol analogue **10i**. Combined with their excellent ligand efficiencies, benzylthioureas could potentially serve as lead compounds for further drug design such as structure-based drug design.

Acknowledgements

The authors thank Ms. Yasuko Watanabe for her excellent technical assistance in chemical synthesis. This work was supported by the grant entitled, "Drug Discovery Program" from Pharma Valley Center, Shizuoka Prefecture, Japan.

Supplementary data

Supplementary data associated with this article can be found, in the online version, at doi:10.1016/j.bmcl.2010.07.025.

References and notes

1. Takikawa, O. *Biochem. Biophys. Res. Commun.* **2005**, *338*, 12.
2. Munn, D. H.; Mellor, A. L. *J. Clin. Invest.* **2007**, *117*, 1147.
3. Sono, M.; Roach, M. P.; Coulter, E. D.; Dawson, J. H. *Chem. Rev.* **1996**, *96*, 2841.
4. Botting, N. P. *Chem. Soc. Rev.* **1995**, *24*, 401.
5. Sono, M.; Hayaishi, O. *Biochem. Rev.* **1980**, *50*, 173.
6. Uyttenhove, C.; Pilotte, L.; Theate, I.; Stroobant, V.; Colau, D.; Parmentier, N.; Boon, T.; van den Eynde, B. *Nat. Med.* **2003**, *9*, 1269.
7. Guillemin, G. J.; Brew, B. J.; Noonan, C. E.; Takikawa, O.; Cullen, K. M. *Neuropath. Appl. Neurobiol.* **2005**, *31*, 395.
8. Fujigaki, H.; Saito, K. *Int. Congr. Ser.* **2007**, *1304*, 314.
9. Potula, R.; Poluektova, L.; Knipe, B.; Chrastil, J.; Heilman, D.; Dou, H.; Takikawa, O.; Munn, D. H.; Gendelman, H. E.; Persidsky, Y. *Blood* **2005**, *106*, 2382.
10. Munn, D. H.; Shafizadeh, E.; Attwood, J. T.; Bondarev, I.; Pashine, A.; Mellor, A. L. *J. Exp. Med.* **1999**, *189*, 1363.
11. Okamoto, A.; Nikaido, T.; Ochiai, K.; Takakura, S.; Saito, M.; Aoki, Y.; Ishii, N.; Yanaihara, N.; Yamada, K.; Takikawa, O.; Kawaguchi, R.; Isonishi, S.; Tanaka, T.; Urashima, M. *Clin. Cancer Res.* **2005**, *11*, 6030.
12. Brandacher, G.; Perathoner, A.; Ladurner, R.; Schneeberger, S.; Orbist, P.; Winkler, C.; Werner, E. R.; Werner-Felmayer, G.; Weiss, H. G.; Gobel, G.; Margreiter, R.; Konigsrainer, A.; Fuchs, D.; Amberger, A. *Clin. Cancer Res.* **2006**, *12*, 1144.
13. Cady, S. G.; Sono, M. *Arch. Biochem. Biophys.* **1991**, *291*, 326.
14. Peterson, A. C.; Migawa, M. T.; Martin, M. J.; Hamaker, L. K.; Czerwinski, K. M.; Zhang, W.; Arend, R. A.; Fisette, P. L.; Ozaki, Y.; Will, J. A.; Brown, R. R.; Cook, J. M. *Med. Chem. Res.* **1994**, *3*, 531.
15. Muller, A. J.; Scherle, P. A. *Nat. Rev. Cancer* **2006**, *6*, 613.
16. Gaspari, P.; Banerjee, T.; Malachowski, W. P.; Muller, A. J.; Prendergast, G. C.; DuHadaway, J.; Bennett, S.; Donovan, A. M. *J. Med. Chem.* **2006**, *49*, 684.
17. Kumar, S.; Malachowski, W. P.; DuHadaway, J. B.; LaLonde, J. M.; Carroll, P. J.; Jaller, D.; Metz, R.; Prendergast, G. C.; Muller, A. J. *J. Med. Chem.* **2008**, *51*, 1706.
18. Carr, G.; Chung, M. K. W.; Mauk, A. G.; Andersen, R. J. *J. Med. Chem.* **2008**, *51*, 2634.
19. Kumar, S.; Jaller, D.; Patel, B.; LaLonde, J. M.; DuHadaway, J. B.; Malachowski, W. P.; Prendergast, G. C.; Muller, A. J. *J. Med. Chem.* **2008**, *51*, 4968.
20. Yue, E. W.; Douty, B.; Wayland, B.; Bower, M.; Liu, X.; Leffet, L.; Wang, Q.; Bowman, K. J.; Hansbury, M. J.; Liu, C.; Wei, M.; Li, Y.; Wynn, R.; Burn, T. C.; Koblish, H. K.; Fridman, J. S.; Metcalf, B.; Scherle, P. A.; Combs, A. P. *J. Med. Chem.* **2009**, *52*, 7364.
21. Zheng, X.; Koropatnick, J.; Li, M.; Zhang, X.; Ling, F.; Ren, X.; Hao, X.; Sun, H.; Vladau, C.; Franek, J. A.; Febg, B.; Urquhart, B. L.; Zhong, R.; Freeman, D. J.; Garcia, B.; Min, W.-P. *J. Immunol.* **2006**, *177*, 5639.
22. IDO activity was determined as follow. In brief, the standard reaction mixture (200 μL) contained 50 mM KPB (pH 6.5), 20 mM ascorbic acid (neutralized with NaOH and HCl), 100 μg/mL catalase, 10 μM methylene blue, 200 μM L-tryptophan, 5 nM recombinant human IDO, and DMSO solution of the compound (4 μL). The reaction was carried out at 37 °C for 60 min and stopped by the addition of 40 μL of 30% (w/v) CCl_3COOH. After heating at 50 °C for 15 min, the reaction mixture was centrifuged at 15000g for 5 min. The supernatant (150 μL) was transferred into a well of a 96-well microplate and mixed with 150 μL of 2% (w/v) *p*-dimethylaminobenzaldehyde in acetic acid. The yellow pigment derived from kynurenine was measured at 490 nm using a SPECTRAmax M5SK microplate reader (Molecular Devices).
23. Matter, H.; Nazaré, M.; Güssregen, S.; Will, D. W.; Schreuder, H.; Bauer, A.; Urmann, M.; Ritter, K.; Wagner, M.; Wehner, V. *Angew. Chem., Int. Ed.* **2009**, *48*, 2911.
24. Hopkins, A. L.; Groom, C. R.; Hopkins, A. A. *Drug Discovery Today* **2004**, *9*, 430.

25. Kynurenine production in A431 cells was determined as follows. In brief, A431 cells (2.0×10^5 cells/mL) were seeded in a 96-well culture plate (100 μL/well) and grown overnight. Serial DMSO dilutions of compounds in a total volume of 100 μL culture medium including tryptophan and human IFN-γ (5 ng/mL final concentration) per well were added into wells containing the cells. After an additional 24 h of incubation, 200 μL/well of a mixed solution of 7% (v/v) aqueous CCl_3COOH and 2% (w/v) *p*-dimethylaminobenzaldehyde in acetic acid (2:5) was added into each well. The yellow color derived from kynurenine was measured at 460 nm using a SPECTRAmax M5SK microplate reader (Molecular Devices).
26. A431 cells were precultured for 24 h. The medium was replaced with fresh medium and the cells were stimulated with or without IFN-γ (5 ng/ml) and the compound **3d** was treated for 24 h. After the treatment, culture media and cell extracts were collected, IDO and α-tubulin were detected by western blot analysis.
27. Hou, D.-Y.; Muller, A. J.; Sharma, M. D.; DuHadaway, J.; Banerjee, T.; Johnson, M.; Mellor, A. L.; Prendergast, G. C.; Munn, D. H. *Cancer Res.* **2007**, *67*, 792.
28. Lu, C.; Lin, Y.; Yeh, S.-R. *J. Am. Chem. Soc.* **2009**, *131*, 12866.
29. Sono, M.; Cady, S. G. *Biochemistry* **1989**, *28*, 5392.
30. Sugimoto, H.; Oda, S.-i.; Otsuki, T.; Hino, T.; Yoshida, T.; Shiro, Y. *Proc. Natl. Acad. Sci. U.S.A.* **2006**, *103*, 2611.

SEMINAR セミナー

インドールアミン酸素添加酵素(IDO)の病態生理学的意義と阻害剤の開発

滝川　修
Osamu TAKIKAWA
国立長寿医療センターラジオアイソトープ管理室室長

横山祐作
Yuusaku YOKOYAMA
東邦大学薬学部教授

1 はじめに

食物由来のトリプトファン(Trp)の95%以上は，キヌレニン(Kyn)経路で代謝される.* この主要代謝経路を開始する酵素として，インドールアミン酸素添加酵素(IDO；indoleamine 2, 3-dioxygenase)とTrp酸素添加酵素(TDO；tryptophan 2, 3-dioxygenase)が存在することが明らかにされている.[1] 最近の研究により，IDOで開始されるTrp代謝が多様な疾病に関与していることが解明され，特にがん，アルツハイマー病，敗血症，老人性白内障などの予防，あるいは治療を目指した新たな分子標的として注目されている(表1).[2] 本稿では，IDOに関する最近のデータと，現在までに報告されたIDO阻害剤と我々が開発した化合物について概説する.

2 がんが誘発する抑制性免疫のメカニズムとIDO

がん細胞は日々絶え間なく発生しているものの，免疫システムがこれを常に監視し駆除しているといわれている.[3] こうした「抗がん免疫」は，主にCD8陽性キラーT細胞やCD4陽性ヘルパーT細胞，抗体などにより構成され，がんを特異的に認識し効率よく傷害する．しかし生体には，制御性T細胞(Treg)などに代表される「抑制性免疫」が存在し，免疫を負に調節する役割を負っている．がん組織が抑制性免疫を局所的に誘発することが最近明らかになり，がんが，抗がん免疫による認識や攻撃を回避し増大・転移・再発を続ける上での重要なメカニズムの1つとして理解されている.

がん誘導性抑制性免疫は，Tregや抑制性分子(TGF-βなどのサイトカイン類，STAT 3，IDOの転写因子・酵素など)により構築されることも明らかになってきている．なかでもIDOは，がん細胞と抑制性樹状細胞において高発現し，がん誘導性抑制性免疫において最も重要なエフェクター分子として機能している.[4] 事実，漿液性卵巣がん,[5] 子宮体がん,[6] 大腸がん,[7] 急性骨髄白血病[8]について，IDO発現の高いがんほど予後不良であることが示されている．したがってIDOを阻害することにより，がんを取り巻く抑制性免疫が解除され，その増殖抑制や転移・再発の阻止といった臨床効果が期待できる.[9,10]

表1　IDOで開始されるTrp代謝異常が増悪因子である疾病

疾病	増悪メカニズム
がん	局所的Trp枯渇及び代謝産物による免疫抑制作用
アルツハイマー病	神経毒キノリン酸の産生
敗血症	全身性Trp枯渇による体タンパク質の崩壊とセロトニン合成低下
老人性白内障	Trp代謝産物(紫外線フィルター)による水晶体タンパク質の加齢性変性

＊　キヌレニン経路についての用語解説は，214頁参照.

3 アルツハイマー病とIDO

アルツハイマー病(AD)は加齢に伴い増加する神経変性疾患であり，高齢化が進む先進国において急増しており，その予防法・治療法の開発は喫緊の社会的課題となっている．ADはアミロイドβペプチド(Aβ)が凝集した老人斑の蓄積に加え，微小管関連タンパク質の1つであるタウが，異常重合した神経原線維変化の形成，さらに領域特性のある神経細胞の脱落を特徴とする．さらに「炎症」が神経変性に関与していることが示唆されており，老人斑に集積したグリア細胞が産生する炎症性サイトカインや活性酸素等による神経変性作用が，「炎症」の本体ではないかと考えられている．

著者らは，種々の炎症性疾患で強く誘導されるIDOと，その代謝産物で興奮性神経毒性を有するキノリン酸(QA)に注目し，ヒトAD剖検脳を精査した結果，老人斑に集積した活性化ミクログリアで異常なIDO発現とQAの蓄積を見いだした.[11] また脳でAβを過剰発現し，老人斑を蓄積するADモデルマウス(Tg 2576)でIDO発現を検討した結果，老人斑に集積したミクログリアにはIDO発現及びQA蓄積は認められないが，起炎剤LPS(リポ多糖)を末梢投与し脳内の「炎症」を増強した時に，初めてIDO誘導及びQA蓄積が生じることを見いだした．以上の結果は，老人斑に集積したミクログリアが，その主要構成成分であるAβによる刺激に加え，脳内の「炎症」が加わったときに強く活性化され，Trp代謝異常を惹起することを示唆している．

この仮説を，ミクログリアのモデルとして汎用されるマクロファージ系細胞株や末梢血単球で検証した結果，Aβと炎症性サイトカインの1つであるIFN-γとの相乗的な刺激でIDOが強誘導されることを発見した.[12] この相乗作用は，神経毒性の本体と考えられているAβ1-42に特異的であり，弱毒性を示すAβ1-40は無効であった．これらの知見は，ADの危険因子が老化や感染症であり，いずれの因子も脳内の炎症性サイトカインを増加させることから，ADの病態を理解する上で重要である．

一方，QAはNMDA(*N*-methyl-D-aspartate)型グルタミン酸受容体を活性化して神経毒性を発揮するが，本受容体の活性化はAβ産生を増大させることが，初代培養神経細胞で報告されている．QAも同様の作用を有していることが予想され，マウスの脳内(海馬内)に直接QAを微量投与して検討した．その結果，投与後7日から海馬のAβ1-40及びAβ1-42共に有意に増加し始め，28日目には数倍にまで顕著に増加した．このQAによるAβ量の増加に一致して海馬の神経細胞は死滅し，海馬容積は約2/3に萎縮した(図1)．これらの事実から，ADでは活性化ミクログリアが産生するQAは神経細胞死を起こし，これにより増加したAβが，2次的に周囲の神経細胞を傷害すると考えられる．このよ

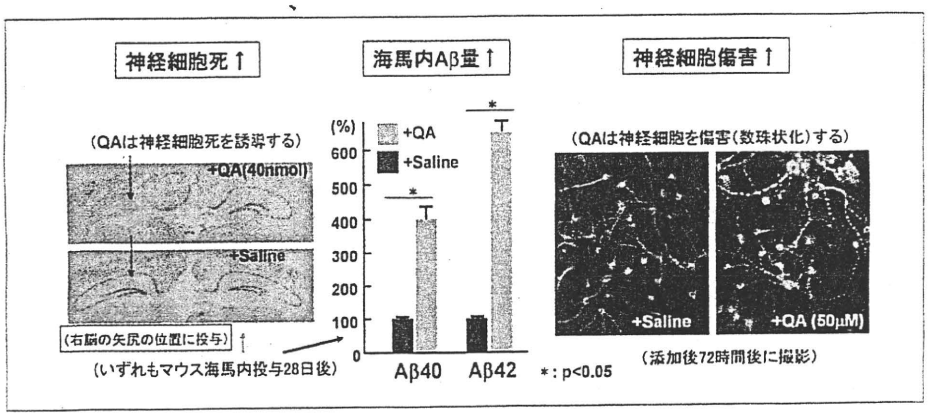

図1 キノリン酸(QA)による神経細胞死とAβレベルの増加

正常マウス海馬内(C 57 BL/6，8週齢，オス)のQA(40 nmol)の1回投与により，海馬の神経細胞はほとんど死滅し，同時にAβレベルが数倍に蓄増する．また，マウスの初代培養神経細胞にQAを添加するとbeading(数珠状)化し，傷害を受けている様子を形態学的に捉えることができる(滝川ら，未発表データ)．

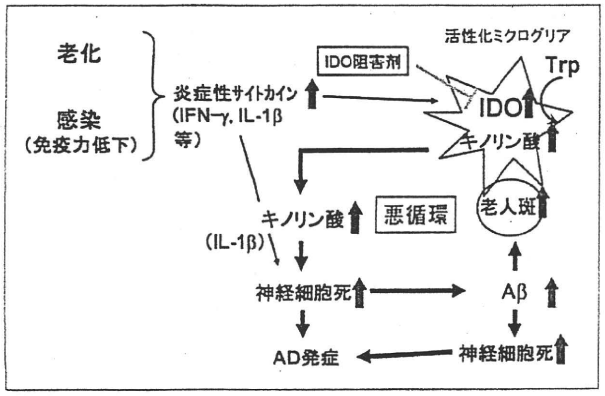

図2 アルツハイマー病(AD)の発症機構におけるIDOの役割(仮説)

ミクログリアで誘導されたIDOが引き金となって，神経毒QAが産生される．QAは神経細胞を傷害し，Aβの産生を促進する．このAβは，更に新たなミクログリアを活性化すると同時に，神経細胞死を起こすという悪循環を形成する．QAの神経毒性は，炎症性サイトカインIL-1βによって増強することも，最近明らかにされている．[10]

うにIDOは，神経細胞死による脳萎縮を特徴とするADに，直接的に関与している可能性が極めて高い．したがってIDO阻害薬は，ADの画期的な根本治療薬となることが期待される(図2)．

4 敗血症とIDO

高齢者に多い敗血症(敗血症性ショック)は死亡率の高い病気であり，炎症性サイトカインストームによる多臓器不全が，その死亡原因とされている．著者らは，LPS投与による敗血症のマウスモデルを作製し解析した結果，敗血症では全身性にIDOが誘導されTrpが大量に代謝されるため，血中Trpレベルが正常の50%近くまで低下し，全身性の枯渇状態になることが分かった．[11] この状態では，Trpレベルを正常レベルに戻そうとする生体防御反応としてタンパク質の異化亢進を招く．特に重感染症ではアルブミンの分解が促進され，浸透圧の維持に支障を来し危険な状態に陥ると予想される．

また，脳内のセロトニン合成は血中のTrpレベルに依存するため，敗血症ではセロトニン不足が生じており，観察される神経機能不全はIDO誘導によるTrp枯渇が一因となっている可能性が高い．したがってIDO阻害剤は，これらTrp枯渇で生じる全身性機能不全を阻止し，従来の抗生剤の治療効果を格段に高めることができると期待される．

5 老人性白内障とIDO

老人性白内障は，眼の水晶体が徐々に黄化混濁し視力が低下する疾病であり，75歳以上の高齢者の罹患率は50%以上である．根本治療薬はなく，手術で水晶体を人工レンズに置換することが唯一の治療法である．本疾病は水晶体の構成成分であるクリスタリンタンパク質の変性がその原因であるが，その変性はクリスタリンタンパク質の酸化(SH基の-SS-結合形成など)，グリコシル(糖)化，構成アミノ酸のL体からD体への異性化，紫外線フィルターによる修飾を伴うことが知られている．なかでも紫外線フィルターによるクリスタリンタンパク質の修飾は，加齢に伴い指数関数的に増大し，その変性の程度は白内障の罹患率によく一致する．

また，紫外線フィルターが活性酸素を産生することから，クリスタリンタンパク質の酸化に関与し得ること，さらにグリコシル化の程度と水晶体の混濁の程度が一致しないことから，紫外線フィルターのクリスタリンタンパク質への結合(図3)が，レンズタンパク質の黄化混濁の主たる原因である可能性が高いと考えられている．[13] この紫外線フィルターの実体は，IDOによりTrpから生合成されるKyn，3OHKyn，3OHKynグリコシドなどであり，ヒト水晶体に高濃度含まれている．通常は水晶体に存在するグルタチオンが，反応性に富む紫外線フィルターの脱アミノ中間体と自ら反応することにより，クリスタリンタンパク質との反応を阻止しているが，加

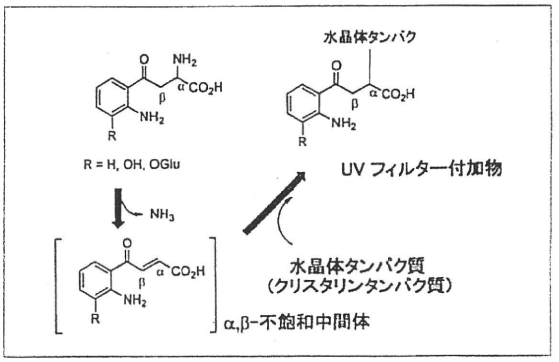

図3 紫外線フィルターとクリスタリンタンパク質の反応

紫外線フィルターであるKyn誘導体の脱アミノ反応で生じる中間体は，クリスタリンタンパク質と反応性し複合体を形成する．

齢に伴いグルタチオンレベルが低下するためタンパク質変性が進行すると考えられる．したがって，紫外線フィルターの生合成を抑制することで老人性白内障の進行を遅延させることが可能であり，IDO阻害剤は新規の老人性白内障薬として期待される．

6 阻害剤の開発

これまで述べてきたように，IDO阻害剤は多くの疾病の根本的治療薬となる可能性がある．しかしIDO阻害剤は，ごく最近まで強い活性を有する化合物が知られていなかった．2009年になって，強い阻害剤が相次いで発表された．阻害剤の歴史的背景と現在までに発表された阻害剤，及び我々が関与している阻害剤の開発について述べる．

IDOの阻害剤として，活性がそれほど強くない*N*-methyltryptophan(1)が1991年に見いだされ，[15] ごく最近まで，この化合物が阻害剤の標準化合物として，多くのIDOに関する生物学的意義に関する研究がなされてきた．その後2005年に，より高い活性の*N*-methylthiohydantointryptophan(MTH-Trp，2)が報告[16]された．この頃より，IDOの生理学的意義や分子標的としての重要性が認識され，数多くの阻害剤が報告されるようになった．ここでは，競合的阻害剤と非競合的阻害剤に分類して，注目される阻害剤を選んで紹介する(図4)．

1. 競合的阻害剤

上で述べた1や2も競合阻害剤である．Gasparらは，植物からphytoalexinとして単離されたbrassinin(4)が比較的強い活性を有していることを見いだした．彼らは詳細な構造活性相関も検討しており，dithiocarbamate部分が活性発現に重要であることを見いだしている．[17] 同じ競合的阻害剤であるMTH-Trp(2)との関係から興味深い．ごく最近，Yueらによって4-amino-1,2,5-oxadiazole-3-carboximidamide誘導体(5)に非常に強い競合的阻害剤が報告された．[18] これは，今までに報告されている他の競合的阻害剤とは異なりインドール環を有していないユニークな構造である．コンピュータによるドッキングスタディーによって，オキシム部分の水酸基が，IDO中のFeと配位結合を有することが重要であることが示唆されている．さらにこの化合物は，酵素に対する阻害活性ばかりでなく，がん細胞であるHeLaの増殖を抑制し，担がんマウスの血漿中のKyn濃度を抑制することも報告しており，医薬品のリード化合物として期待される．

2. 非競合的阻害剤

活性が比較的強い化合物として，1993年にPetersonらによって3-butyl-β-carbolin誘導体(6)が報告[19]されたが，最近になって強い活性を有する化合物が多く報告されている．本稿では，特に強い活性を有するものに絞って紹介する．

Carrらはmarine spongeから単離されたalkaloidが強いIDO阻害活性を有することにヒントを得，より単純な化合物(7)に強い阻害活性を有することを見いだした．[20] 最も強い活性を持つ非競合阻害剤として，キノン誘導体(8)がKumarらによって報告された．[21] 彼らは，ビタミンK(9)も比較的強い阻害活性を有することから，quinone構造が活性の発現には必要であると予想している．

7 IDOの構造と作用機序

IDOはP 450などと同様に，ヘムを有する酸素添加酵素であるが，40年以上も前に発見された酵素であるにもかかわらず，詳細な反応機構に関して不明であった．この原因は，この酵素の構造に関する情報がほとんどなかったことと，その反応形式が他

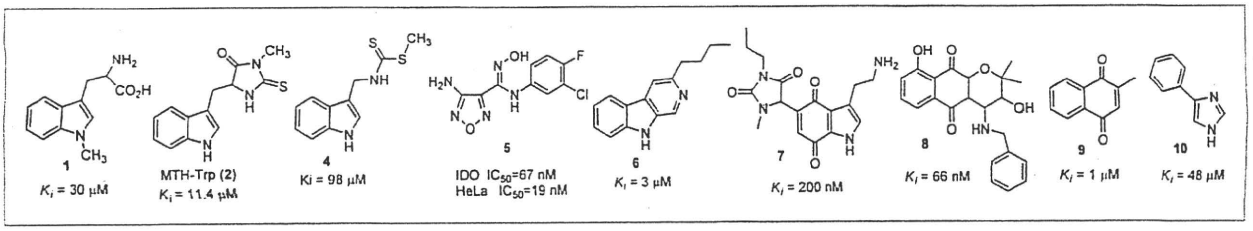

図4 阻害剤の構造と阻害活性

の酸素添加酵素の反応形式と大きく異なっていたことが原因である．

しかし，ごく最近になって，弱い非拮抗阻害剤として知られている4-phenylimidazole(10)と錯体を形成したIDOの結晶のX線構造が報告された．[22] 活性部位に存在するserine，tyrosine，histidineといった極性アミノ酸の活性発現に対する役割は大きくないことも，構造の解析やポイントミューテーションの実験から明らかになっている．また最近，諸熊らによって詳細な計算化学的考察がなされており，活性部位の構造，反応機構も明らかになりつつある．[23]

8 我々のグループ阻害剤の開発

我々は，Trpの生合成類似のルート，すなわちインドールとセリンから直接Trp誘導体を得る実用的合成法を初めて報告した．[24] Trp誘導体がIDO阻害剤としての可能性を有するということから，この反応を利用してTrpアナログを合成し，新しいIDO阻害剤を見いだそうと計画した．ベンズTrp類が，IDO阻害剤としての可能性があることが報告されていることから，我々の開発した方法にしたがって，種々のbenztryptophan類の合成を行った(図5)．すなわち，benzindole類(11a～c)をAc_2O存在下酢酸中で加熱した後エステル化を行い，*N*-acetylbenztryptophan類(12a～c)を42～54%の収率で得た．しかし残念ながら，それらの誘導体の活性はそれほど強くなかった．

そこで，MTH-Trp(2)より強い活性を有することを期待して，MTH-benz[*e*]tryptophan(15)の合成を13より2行程で行ったところ(図6，Route A)，若干活性の増大が見られたものの，満足できる活性物質は得られなかった．しかし驚くべきことに，この合成の過程で少量(6%)得られた副生成物(16)は，MTH-Trp(2)よりも強い阻害活性を示した(図7)．この化合物(16)は，同じ出発物質(13)から別途合成により，3行程，総収率71%を得ることで，その構造を確認した(図6，Route B)．

さらに，この合成ルートにより類似体17，18，19の合成も行い(図8)，その阻害活性を測定した．その結果，Trp誘導体17には，それ程強い活性はなかったが，benz[*f*]-，benz[*g*]誘導体18，19には，16と同様に強い活性が見られた(図7)．なお，これらの化合物は，Trp同族体であるにもかかわらず，非拮抗阻害剤であることも判明しており，構造活性相関の観点から興味が持たれる．[25]

9 おわりに

IDOの生体内での役割の重要性は，この1，2年で急速に明らかになりつつあると同時に，多くの疾患の新しい分子標的として急激に注目を浴びつつある．また，X線解析によりタンパク質の構造が明らかになると同時に，活性部位，作用機序の解明も進みつつある．そして，阻害剤の構造活性相関，阻害機構が明らかになり，活性が強い化合物も見いだされつつある．このようなことから，今後IDO阻害剤

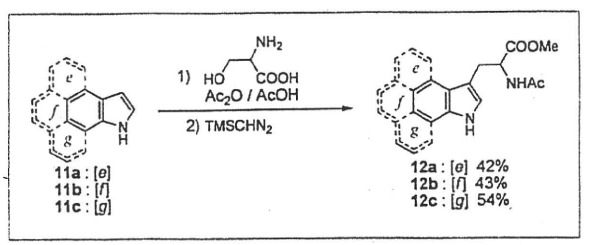

図5 Benztryptophan類の合成

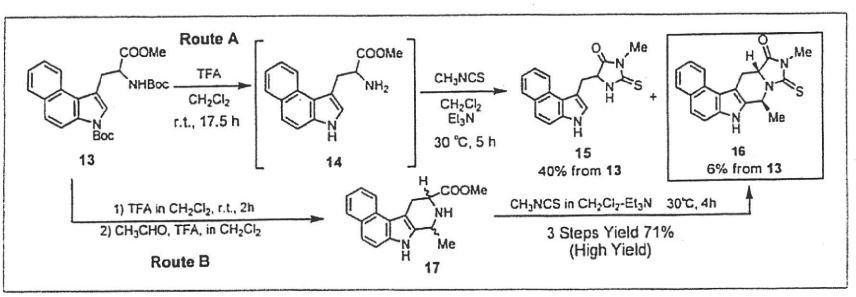

図6 阻害剤の合成ルート

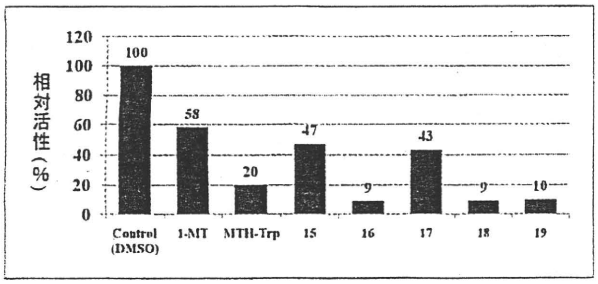

図7　阻害活性：阻害剤の濃度が200 μMの時の相対活性

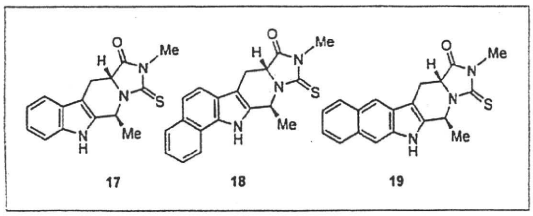

図8　合成した阻害剤の構造

は有望な医薬品としての可能性が開けている．本稿が，新しい医薬品開発の一助となれば本望である．

文　献

1) Takikawa O. *et al*., *J. Biol. Chem*., 338, 12 (1986).
2) Takikawa O., *Biochem. Biophys. Res. Commun*., 338, 12 (2005).
3) Swann J. B., Smyth M. J., *J. Clin. Invest*., 117, 1137 (2007).
4) Munn D. H., Mellor A. L., *J. Clin. Invest*., 117, 1147 (2007).
5) Okamoto A. *et al*., *Clin. Cancer Res*., 11, 6030 (2005).
6) Ino K. *et al*., *Clin. Cancer Res*., 14, 2310 (2008).
7) Brandacher G. *et al*., *Clin. Cancer Res*., 12, 1144 (2006).
8) Chamuleau M. E. *et al*., *Haematologica*, 93, 1894 (2008).
9) Uyttenhove C. *et al*., *Nature Med*., 9, 1269 (2003).
10) Yoshida N. *et al*., *Clin. Cancer Res*., 14, 7251 (2008).
11) Guillemin G. J. *et al*., *Neuropathol. Appl. Neurobiol*., 31, 395 (2005).
12) Yamada A. *et al*., *J. Neurochem. J. Neurochem*., 110, 791 (2009).
13) Takikawa O. *et al*., *Exp. Eye. Res*., 72, 271 (2001).
14) Stone T. W., Behan W. M., *J. Neurosci. Res*., 85, 1077 (2007).
15) Cady S. G, Sono M., *Arch. Biochem. Biopys*., 291, 326-333 (1991).
16) Muller A. J. *et al*., *Nat. Med*., 11, 312-319 (2005).
17) Gaspari P. *et al*., *J. Med. Chem*., 49, 684-692 (2006).
18) Yue E. W. *et al*., *J. Med. Chem*., 52, 7364-7367 (2009).
19) Peterson A. C. *et al*., *Med. Chem. Res*., 3, 531-544 (1994).
20) Carr G. *et al*., *J. Med. Chem*., 51, 2634-2637 (2008).
21) Kumar S. *et al*., *J. Med. Chem*., 51, 1706-1718 (2008).
22) Sugimoto H. *et al*., *PNAS*, 103, 2611-2616 (2006).
23) Chung L. W. *et al*., *J. Am. Chem. Soc*., 130, 12299-12309 (2008).
24) Yokoyama Y. *et al*., *Euro. J. Org. Chem*., 2004, 1244-1253.
25) 滝川　修ほか，特願 2007-041962.

談話室

USA は省略可?

森田真也
神戸薬科大学助教・ファルマシア支部アドバイザー

英文誌の論文において，試薬や機器の購入先について Nacalai Tesque (Kyoto, Japan) や GE Healthcare (Buckinghamshire, UK) のように都市名と国名を付けて書くことが慣例となっています．しかし，アメリカの会社から購入した場合，Sigma (St. Louis, MO) や Bio-Rad (Hercules, CA) というように都市名と州略号を記載し，USA は省略されていることが多く，そのように書くものだと，これまで思っていました．

ところが先日，英文校正サービスから返ってきた論文原稿を見たところ，Invitrogen (Carlsbad, CA, USA) のように，州略号のあとに USA を記載するように促されていました．そもそも，試薬機器会社の記載形式について触れている論文投稿規定は見たことがありません．そこで，限られた範囲 (主に生化学系雑誌) ではあるのですが調べてみました．

まず，アメリカの学会が編集を行っている *J. Biol. Chem.* や *Biochemistry*, *Mol. Biol. Cell*, *Mol. Pharmacol*., *Am. J. Physiol*., *Biophys. J.* においては，試薬機器会社所在地の記載において USA という表記は省略されており，著者の所属においても USA は省略されています．しかし，*FASEB J.* では USA が表記されています．また，ヨーロッパの学会が編集している *FEBS J.* や *EMBO Rep.* では，USA が省略されずに記載されています．

そして，日本薬学会が編集している *Biol. Pharm. Bull.* 並びに日本生化学会の *J. Biochem.* では，会社所在地の USA は明記されています．一方，日本分子生物学会の *Genes Cells* や日本農芸化学会の *Biosci. Biotechnol. Biochem.* では，会社所在地の USA は省略されていることが多いようです．もちろん，これらの日本の学会が編集している英文誌で，Japan が省略されていることはありません．

これらは論文の内容や審査には関係ないことなのですが，執筆時のご参考までに．

注：このような傾向が雑誌によって見られましたが，あてはまらない論文もあります．会社の所在地を書いていない論文も多くあります．

Molecular Neurodegeneration

BioMed Central
The Open Access Publisher

Extracellular and intraneuronal HMW-AbetaOs represent a molecular basis of memory loss in Alzheimer's disease model mouse

Molecular Neurodegeneration 2011, **6**:20 doi:10.1186/1750-1326-6-20

Ayumi Takamura (ayumi@cc.hirosaki-u.ac.jp)
Yasuhide Okamoto (y-okamoto@immunas.co.jp)
Takeshi Kawarabayashi (tkawara@cc.hirosaki-u.ac.jp)
Tatsuki Yokoseki (t-yokoseki@immunas.co.jp)
Masao Shibata (shibata@inacatv.ne.jp)
Akihiko Mouri (amouri@ccmfs.meijo-u.ac.jp)
Toshitaka Nabeshima (tnabeshi@ccmfs.meijo-u.ac.jp)
Hui Sun (sunhuidalian@gmail.com)
Koji Abe (abekabek@cc.okayama-u.ac.jp)
Tsuneo Urisu (urisu@ims.ac.jp)
Naoki Yamamoto (naokisan@ph.ritsumei.ac.jp)
Mikio Shoji (mshoji@cc.hirosaki-u.ac.jp)
Katsuhiko Yanagisawa (katuhiko@ncgg.go.jp)
Makoto Michikawa (michi@ncgg.go.jp)
Etsuro Matsubara (etsuro@cc.hirosaki-u.ac.jp)

ISSN 1750-1326

Article type Research article

Submission date 13 August 2010

Acceptance date 6 March 2011

Publication date 6 March 2011

Article URL http://www.molecularneurodegeneration.com/content/6/1/20

http://www.molecularneurodegeneration.com/info/instructions/

For information about other BioMed Central publications go to

http://www.biomedcentral.com/

Extracellular and intraneuronal HMW-AbetaOs represent a molecular basis of memory loss in Alzheimer's disease model mouse

Ayumi Takamura[1,2], Yasuhide Okamoto [1,3], Takeshi Kawarabayashi[2], Tatsuki Yokoseki[3], Masao Shibata[3], Akihiko Mouri[4], Toshitaka Nabeshima[4], Hui Sun[1], Koji Abe[5], Tsuneo Urisu[6], Naoki Yamamoto[1], Mikio Shoji[2], Katsuhiko Yanagisawa[1], Makoto Michikawa[1] and Etsuro Matsubara[*1,2]

[1] Department of Alzheimer's Disease Research, Research Institute, National Center for Geriatrics and Gerontology, Aichi, Japan, [2] Department of Neurology, Institute of Brain Science, Hirosaki University Graduate School of Medicine, Aomori, Japan, [3] Immunas Pharma Incorporation, Kanagawa, Japan, [4] Department of Chemical Pharmacology, Graduate School of Pharmaceutical Sciences, Meijo University, Aichi, Japan, [5] Department of Neurology, Okayama University School of Medicine, Okayama, Japan, [6] Department of Life and Coordination-Complex Molecular Science, Institute for Molecular Science, Aichi, Japan

Email: AT: ayumi@cc.hirosaki-u.ac.jp; YO: y-okamoto@immunas.co.jp; TK: tkawara@cc.hirosaki-u.ac.jp; TY: t-yokoseki@immunas.co.jp; MS: shibata@inacatv.ne.jp; AM: amouri@ccmfs.meijo-u.ac.jp; TN: tnabeshi@ccmfs.meijo-u.ac.jp; HS: sunhuidalian@gmail.com; KA: abekabek@cc.okayama-u.ac.jp; TU: urisu@ims.ac.jp; NY: naokisan@ph.ritsumei.ac.jp; MS: mshoji@cc.hirosaki-u.ac.jp; KY: katuhiko@ncgg.go.jp; MM: michi@ncgg.go.jp; EM*: etsuro@cc.hirosaki-u.ac.jp.

* Corresponding author

Abstract

Background: Several lines of evidence indicate that memory loss represents a synaptic failure caused by soluble amyloid β (Aβ) oligomers. However, the pathological relevance of Aβ oligomers (AβOs) as the trigger of synaptic or neuronal degeneration, and the possible mechanism underlying the neurotoxic action of endogenous AβOs remain to be determined.

Results: To specifically target toxic AβOs *in vivo*, monoclonal antibodies (1A9 and 2C3) specific to them were generated using a novel design method. 1A9 and 2C3 specifically recognize soluble AβOs larger than 35-mers and pentamers on Blue native polyacrylamide gel electrophoresis, respectively. Biophysical and structural analysis by atomic force microscopy (AFM) revealed that neurotoxic 1A9 and 2C3 oligomeric conformers displayed non-fibrilar, relatively spherical structure. Of note, such AβOs were taken up by neuroblastoma (SH-SY5Y) cell, resulted in neuronal death. In humans, immunohistochemical analysis employing 1A9 or 2C3 revealed that 1A9 and 2C3 stain intraneuronal granules accumulated in the perikaryon of pyramidal neurons and some diffuse plaques. Fluoro Jade-B binding assay also revealed 1A9- or 2C3-stained neurons, indicating their impending degeneration. In a long-term low-dose prophylactic trial using active 1A9 or 2C3 antibody, we found that passive

immunization protected a mouse model of Alzheimer's disease (AD) from memory deficits, synaptic degeneration, promotion of intraneuronal AβOs, and neuronal degeneration. Because the primary antitoxic action of 1A9 and 2C3 occurs outside neurons, our results suggest that extracellular AβOs initiate the AD toxic process and intraneuronal AβOs may worsen neuronal degeneration and memory loss.

Conclusion: Now, we have evidence that HMW-AβOs are among the earliest manifestation of the AD toxic process in mice and humans. We are certain that our studies move us closer to our goal of finding a therapeutic target and/or confirming the relevance of our therapeutic strategy.

Background

Alzheimer's disease (AD) represents the so-called "storage disorder" of amyloid β (Aβ). The AD brain contains soluble and insoluble Aβ, both of which have been hypothesized to underlie the development of cognitive deficits or dementia [1-3]. The steady-state level of Aβ is controlled by the generation of Aβ from its precursor, the degradation of Aβ within the brain, and transport of Aβ out of the brain. The imbalance among three metabolic pathways results in excessive accumulation and deposition of Aβ in the brain, which may trigger a complex downstream cascade (e.g., primary amyloid plaque formation or secondary tauopathy and neurodegeneration) leading to memory loss or dementia in AD. Accumulated lines of evidence indicate that such a memory loss represents a synaptic failure caused directly by soluble Aβ oligomers (AβOs) [4-6], whereas amyloid fibrils may cause neuronal injury indirectly via microglial activation [7]. Thus, the classical amyloid cascade hypothesis [8] underwent a modification in which the emphasis is switched to the intermediate form of Aß such as AβOs [9-12], rather than fibrillar Aß [7]. If this were the case, therapeutic intervention targeting AβOs may be effective in blocking this pathogenic cascade. The outcome of a recent human AN-1791 trial confirmed that plaque removal did not prevent the progression of neuronal degeneration [13], supporting this hypothesis.